

ОБЪЕДИНЕННЫЙ
ИНСТИТУТ
ЯДЕРНЫХ
ИССЛЕДОВАНИЙ

Дубна

97-50

E9-97-50

J.Feldhaus¹, E.L.Saldin², J.R.Schneider¹,
E.A.Schneidmiller², M.V.Yurkov

METHOD FOR REDUCING
THE RADIATION BANDWIDTH OF AN X-RAY FEL

Submitted to «Photonics West'97», February 8—14, 1997, San Jose, USA

¹HASYLAB at Deutsches Elektronen-Synchrotron (DESY), Notkestrasse 85,
D-22607 Hamburg, Germany

²Automatic Systems Corporation, 443050 Samara, Russia

1997

1 Introduction

In this paper we propose a modification of a single pass X-ray SASE FEL allowing to reduce significantly the bandwidth of the output radiation. The proposed scheme consists of two undulators and an X-ray monochromator located between them (see Fig. 1). The first undulator operates in the linear regime of amplification starting from noise and the output radiation has the usual SASE properties. After the exit of the first undulator the electron is guided through a bypass and the X-ray beam enters the monochromator which selects a narrow band of radiation. At the entrance of the second undulator the monochromatic X-ray beam is combined with the electron beam and is amplified up to the saturation level.

The electron micro-bunching induced in the first undulator should be destroyed prior to its arrival at the second one. This can be achieved because of the finite value of the natural energy spread in the beam and by applying a special design of the electron bypass. At the entrance of the second undulator the radiation power from the monochromator dominates significantly over the shot noise and the residual electron bunching, so that the second stage of the FEL amplifier will operate in the steady-state regime when the input signal bandwidth is small with respect to the FEL amplifier bandwidth.

The monochromatization of the radiation is performed at a low level of radiation power which allows one to use conventional X-ray optical elements for the monochromator design. X-ray grating techniques can be used successfully down to wavelengths of several Å and at shorter wavelengths crystal monochromators could be used. Integral losses of the radiation power in the monochromator are relatively small because grazing incidence optics can be used. The proposed scheme possesses two significant advantages. First, it reveals a perspective to achieve monochromaticity of the output radiation close to the limit given by the finite duration of the radiation pulse and to increase the brilliance of the SASE FEL. Second, shot-to-shot fluctuations of the output radiation power could be reduced to less than 10 % when the second undulator section operates at saturation. Since it is a single bunch scheme, it does not require any special time diagram for accelerator operation.

2 Principle of operation of a two stage SASE FEL

After the first undulator the electron beam is guided through a bypass and the X-ray beam enters the monochromator. The functions of the electron bypass consist in making the path lengths of the electron and the radiation beams equal, and in suppressing the modulation of the electron bunch produced in the first undulator.

Let us consider the simplest non-isochronous scheme of the electron bypass composed of three magnets which is symmetrical with respect to its center. The trajectory of the electron beam in the bypass has the shape of an isosceles triangle with the base equal to L , the distance between the two undulators. The angle adjacent to the base, θ , is considered

to be small, $\theta \ll 1$. We assume that the particles in the electron beam have a Gaussian energy distribution: $f(P) = (\sqrt{2\pi}\sigma_\varepsilon)^{-1} \exp(-P^2/2\sigma_\varepsilon^2)$. Here $P = (\mathcal{E} - \mathcal{E}_0)/\mathcal{E}_0$, σ_ε is the standard deviation, \mathcal{E}_0 is the nominal energy of the particles. We also assume that at the entrance of the bypass the electron bunch's density and energy are modulated with wavelength λ equal to that of the FEL radiation. At the exit of the bypass the modulations are suppressed by a factor of

$$D = \exp(-4\pi^2\sigma_\varepsilon^2\theta^4 L^2/2\lambda^2). \quad (1)$$

Let us consider the specific numerical example with $\sigma_\varepsilon \simeq 0.1\%$, $\lambda \simeq 6$ nm, $\theta \simeq 1^\circ$ and $L \simeq 10^3$ cm. According to expression (1), the electron beam modulations are suppressed by a factor of $D = \exp(-5000000)$. Thus, the initial modulation of the electron beam at the entrance into the second undulator is given by the shot noise only.

To provide effective operation of a two-stage SASE FEL, the input radiation power $P_{in}^{(2)}$ at the entrance to the second undulator must exceed significantly the effective power, P_{shot} , of shot noise. When the power gain in the first undulator is equal to $G^{(1)}$ and the transmission factor of the monochromator is equal to T_m , one can write: $P_{in}^{(2)}/P_{shot} = G^{(1)}T_m$. The transmission factor $T_m = R_m K_s$ is defined by the product of the integral reflection coefficient R_m of the mirrors and the dispersive element, and the coefficient K_s describing the radiation losses at the exit slit of the monochromator: $K_s = (\Delta\lambda/\lambda)_m/(\Delta\lambda/\lambda)_{SASE}$, where $(\Delta\lambda/\lambda)_m$ is the resolution of the monochromator and $(\Delta\lambda/\lambda)_{SASE}$ is the radiation bandwidth of the SASE FEL at the exit of the first undulator. As a result, one obtains the following criterium for the power gain in the first undulator: $P_{in}^{(2)}/P_{shot} = G^{(1)}R_m K_s \gg 1$.

In addition, the resolution of the monochromator should satisfy the following conditions: $\lambda/\pi\sigma_z < (\Delta\lambda/\lambda)_m \ll (\Delta\lambda/\lambda)_{SASE}$. The lower limitation on $(\Delta\lambda/\lambda)_m$ is due the fact that the length of the longitudinal coherence of the radiation can not be larger than the length of the electron bunch, σ_z .

The amplification process in the first undulator leads to an energy modulation in the electron beam. After passing the bypass this energy modulation transforms into additional energy spread in the electron beam: $\Delta\sigma_\varepsilon \simeq \rho[G^{(1)}/G_{sat}(SASE)]^{1/2}$, where ρ is the saturation parameter [3,4], $G_{sat}(SASE)$ is the power gain of SASE FEL at saturation. For effective operation of the second stage of the FEL amplifier, this induced energy spread should be small; $\sigma_\varepsilon^2 \ll \rho^2$, which leads to condition: $G^{(1)} \ll G_{sat}(SASE)$. This relation means that the first stage of the SASE FEL must operate in a linear high-gain regime.

When optimizing the two-stage FEL one should take into account significant shot-to-shot fluctuations at the exit of the monochromator. The first undulator operates in the SASE linear regime. Therefore, probability for a certain power $P(t)$ at the time t at the output of the first undulator is given by the well-known Rayleigh probability density function

$$w(P)dP = \exp(-P/\langle P \rangle)dP/\langle P \rangle$$

The monochromator does not change this distribution since it is merely a linear filter. However, it changes the characteristic time scale to $(\lambda/c)(\Delta\lambda/\lambda)_m^{-1}$ because its bandwidth $(\Delta\lambda/\lambda)_m$ is considerably smaller than that the FEL amplifier. This also ensures that the second amplifier works in the steady state regime. We have actually tested our FEL simulations by calculating a histogram of intensities from the simulated data (see Fig. 2). Fig. 3 shows that this distribution agrees very well with the Rayleigh probability density function. It is seen from Fig. 3 that if the radiation power at the exit of the monochromator (averaged over shot-to-shot fluctuations) is about of two orders of magnitude higher than the effective power of shot noise, the second stage operates in the steady-state regime with the probability close to unity.

In conclusion to this section we combine all the conditions necessary and sufficient for the effective operation of a two-stage SASE FEL:

$$\begin{aligned} P_{in}^{(2)}/P_{shot} &= G^{(1)}R_m(\Delta\lambda/\lambda)_m/(\Delta\lambda/\lambda)_{SASE} > 10^2, \\ \lambda/\pi\sigma_z &< (\Delta\lambda/\lambda)_m \ll (\Delta\lambda/\lambda)_{SASE}, \\ G^{(1)} &\ll G_{sat}(SASE). \end{aligned} \quad (2)$$

3 Numerical example

The operation of a two-stage SASE FEL is illustrated for the 6 nm option of the SASE FEL which is under construction at DESY (see Table 1) [1]. For our calculations we have used the same parameters for the electron beam and the undulator.

Parameters of the first stage of the SASE FEL are presented in Table 2. It operates in a linear regime with a power gain $G^{(1)} = 10^5$. This value is 1000 times less than the power gain at saturation, $G_{sat}(SASE) \simeq 10^8$ (see Table 1). Spectral characteristics of the output radiation at the exit of the first stage are presented in Fig. 2 (see [6,7]).

The monochromator for the TTF-FEL should be able to select any energy between 50 eV and 200 eV with a resolution $(\Delta\lambda/\lambda)_m \simeq 5 \times 10^{-5}$ in order to resolve the fine structure shown in Fig. 2. The optics needed to couple the radiation in and out of the monochromator would be particularly simple and symmetric if a monochromator design was chosen whose magnification would be independent of wavelength. Therefore, a Rowland circle grating monochromator appears to be ideally suited for this purpose since the magnification of the spherical grating is always unity, independent of wavelength. The specific design of F. Senf et al. [5] has the additional advantage that the distance between the entrance and the exit slit is constant and the directions of the in- and outgoing beams are fixed, leading to a straightforward design as shown schematically in Fig. 4. A first estimation of the transmission shows that a value of the order of 10 % is realistic. For all mirrors we use carbon coatings and grazing angles of incidence of 4° , giving a reflectivity of 90 % for each mirror. Assuming a grating efficiency of 15 % and five mirrors with 90 % reflectivity then gives a total transmission of nearly 9 %.

Table 1

Parameters of the conventional SASE FEL at DESYElectron beam

Energy, \mathcal{E}_0	1000 MeV
Peak current, I_0	2500 A
rms bunch length, σ_z	50 μm
Normalized rms emittance, ϵ_n	2 π mm mrad
rms energy spread	0.1 %
External β -function,	300 cm
rms transverse beam size	57 μm
Number of bunches per train	7200
Repetition rate	10 Hz

Undulator

Type	Planar
Length of undulator, L_w	20 m
Period, λ_w	2.73 cm
Peak magnetic field, H_w	4.97 kGs

Radiation

Wavelength, λ	6.4 nm
Bandwidth, $(\Delta\lambda/\lambda)_{\text{SASE}}$	0.5 %
rms angular divergence	15 μrad
rms spot size	90 μm
autocorrelation time, $\tau_{1/2}$	3 fs
Power average over pulse	5 GW
Flash energy	1.5 mJ
Average power	100 W
Average spectral brilliance	7×10^{22} Phot./ $(\text{sec} \times$ $\text{mrad}^2 \times \text{mm}^2 \times$ 0.1% bandw.)

Table 2

Parameters of the first stage of the two-stage SASE FEL

Mode of operation	SASE, linear amplification
Effective power of shot noise, P_{shot}	100 W
Length of undulator, L_w	12 m
Effective gain, G	10^5
<u>Output radiation</u>	
Wavelength, λ	6.4 nm
Bandwidth, $(\Delta\lambda/\lambda)_{\text{SASE}}$	0.5 %
Autocorrelation time, $\tau_{1/2}$	2 fs
rms spot size	40 μm
rms angular divergence	18 μrad
Peak power	50 MW
Power average over pulse,	10 MW
Flash energy	3 μJ
Average power	0.2 W

Table 3

Parameters of the second stage of the two-stage SASE FEL

Mode of operation	Steady-state, saturation
Input power, $P_{in}^{(2)}$	10^4 W
Length of undulator, L_w	16 m
Gain, G	10^6
<u>Output radiation</u>	
Wavelength, λ	6.4 nm
Bandwidth, $\Delta\lambda/\lambda$	5×10^{-5}
rms angular divergence	$15 \mu\text{rad}$
rms spot size	$90 \mu\text{m}$
Peak power	5.3 GW
Flash energy	1.5 mJ
Average power	100 W
Average spectral brilliance	7×10^{24} Phot./($\text{sec} \times$ $\text{mrad}^2 \times \text{mm}^2 \times$ 0.1 % bandw.)

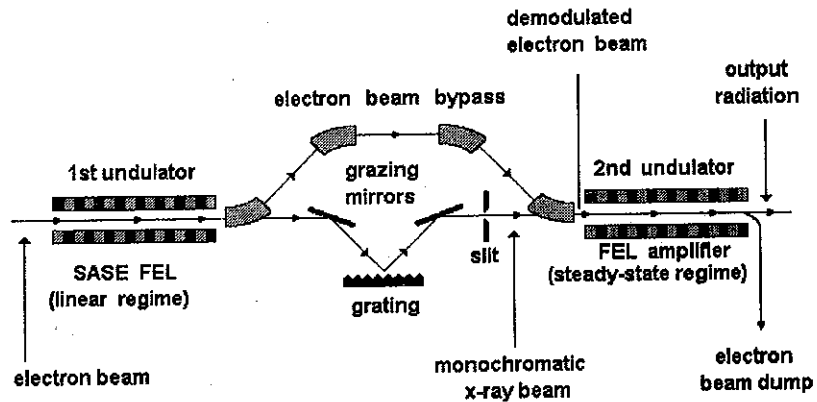


Fig. 1. The principal scheme of a single-pass two-stage SASE X-ray FEL with monochromator.

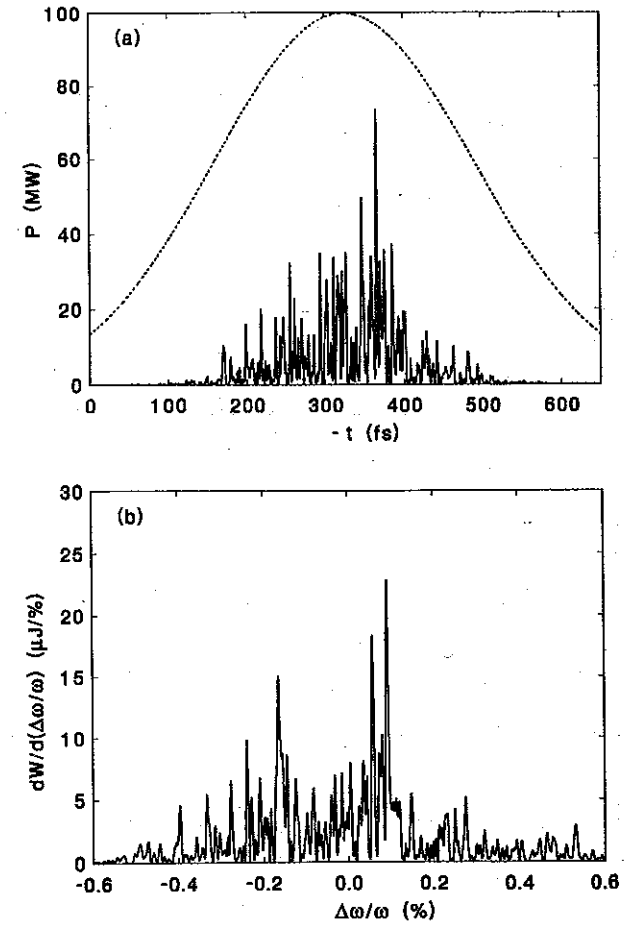


Fig. 2. Temporal (a) and spectral (b) structure of a radiation pulse at the exit of the first undulator. The dashed line presents the corresponding distribution of the electron beam current.

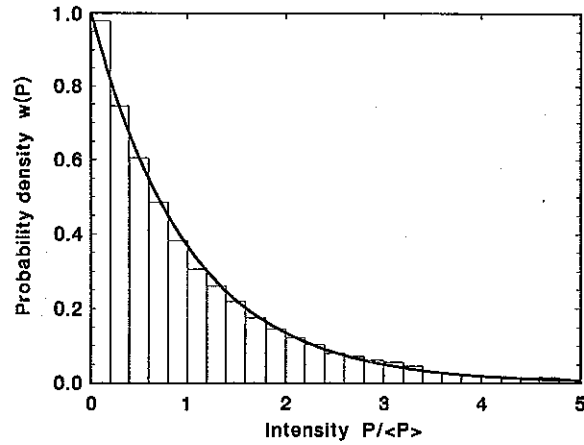


Fig. 3. A histogram of 8000 of intensity points taken over the full radiation pulse length (see Fig. 2). $\langle P \rangle$ denotes the intensity averaged over the radiation pulse. The solid curve represents the Rayleigh probability density function $w(P) = \exp(-P/\langle P \rangle)$.

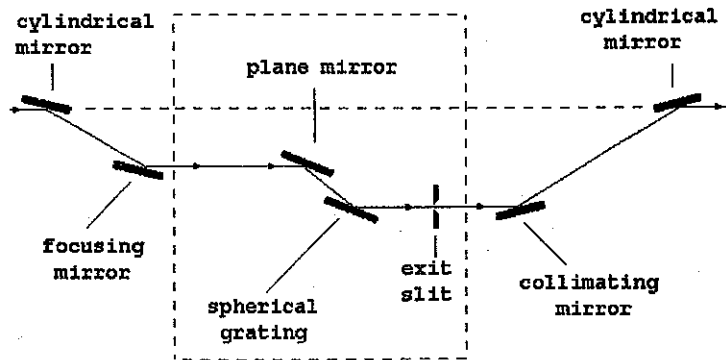


Fig. 4. Layout of a grating monochromator for the TTF FEL (Rowland circle monochromator).

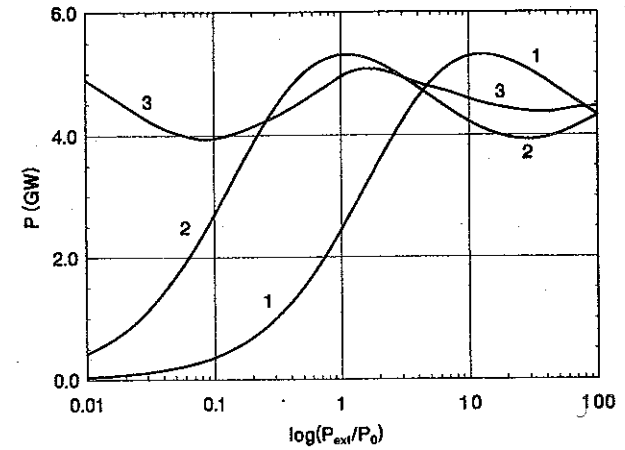


Fig. 5. Dependence of the output power on the input power for the FEL amplifier operating in the steady-state regime, (1): For an undulator length $L_w = 14$ m, (2): $L_w = 16$ m, (3): $L_w = 20$ m. Nominal external power $P_0 = 10$ kW.

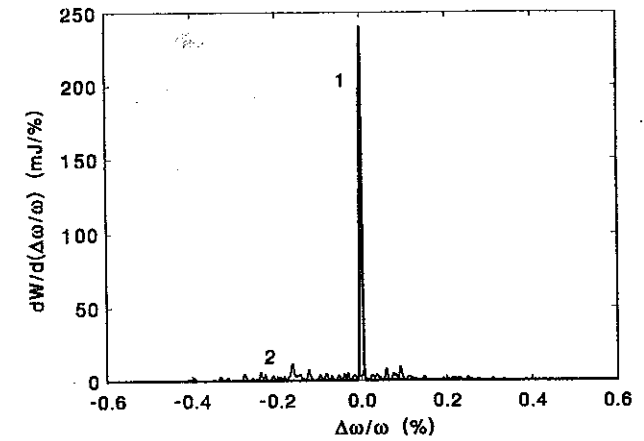


Fig. 6. Spectral distribution (1) of the energy in one radiation pulse of the FEL amplifier operating in the steady-state regime for an input power $P_0 = 10$ kW and an undulator length $L_w = 16$ m (saturation point). Curve (2) presents typical spectrum of conventional SASE FEL operating at saturation.

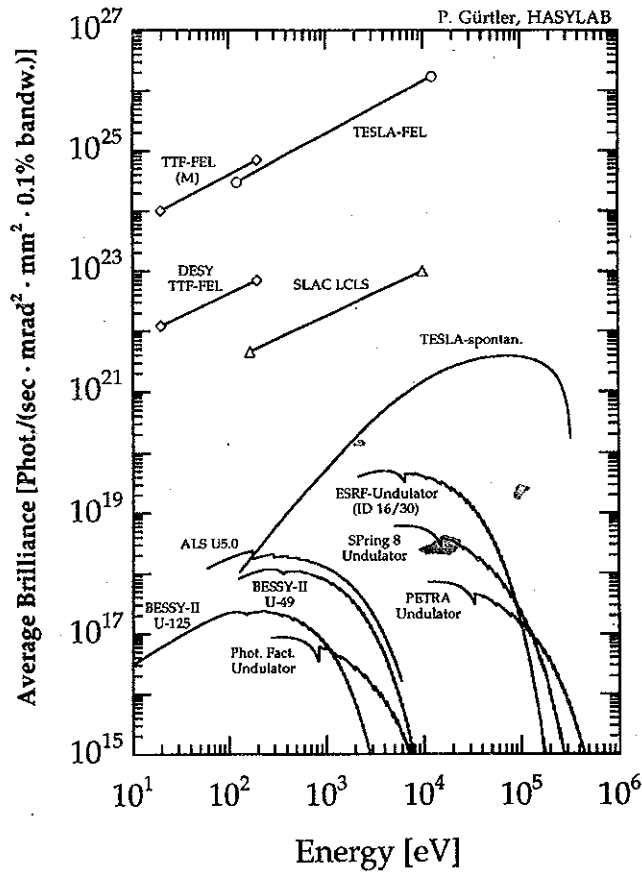


Fig. 7. Average brilliance for different radiation sources. The brilliance for the FEL sources has been calculated according to $B = 4\dot{N}_{ph}/\lambda^2/(\Delta\lambda/\lambda)$.

The parameters of the second stage of the SASE FEL are presented in Table 3. The average value of the input radiation power is 10 kW, which results in a saturation length of 16 m. The quality of the output radiation of the two-stage SASE FEL exceeds significantly that of the conventional SASE FEL (compare Tables 3 and 1). For our numerical example we have chosen such parameters that the seeding of the second stage still works at the power level of few per cent of the average power $\langle P \rangle$. Hence, the probability that the seeding scheme does not work is of the order of few per cent.

The flash energy of the two-stage SASE FEL is close to that of the conventional SASE FEL while the spectral bandwidth is by two orders of magnitude narrower. Thus, the spectral brilliance of the output radiation exceeds the corresponding value of a conventional SASE FEL by two orders of magnitude. In addition, longitudinal coherence of the output radiation over the full radiation pulse (300 fs).

Fig. 5 shows that the value of the output radiation power is rather insensitive to the fluctuations of the input power when the second stage of the FEL amplifier operates near the saturation point. From the Rayleigh probability function we derive that approximately 70% of all pulses at the entrance of second undulator fall within an interval $0.3 < P/\langle P \rangle < 3$, leading to fluctuations of less than 10% at the output of the second undulator according to Fig. 5. Fig. 6 shows comparative results for the energy spectrum of monochromatized and conventional version of SASE FEL at the TESLA Test Facility at DESY. Fig. 7 illustrates perspectives of the proposed method to increase the brilliance of SASE FEL.

References

- [1] "A VUV Free Electron Laser at the TESLA Test Facility at DESY. Conceptual Design Report", DESY print, TESLA-FEL 95-03, Hamburg (1995).
- [2] J. Rossbach, Nucl. Instrum. and Methods **A375**(1996)269.
- [3] R. Bonifacio, C. Pellegrini and L. Narducci, Opt. Commun. **50**(1984)373
- [4] E.L. Saldin, E.A. Schneidmiller and M.V. Yurkov, Phys. Rep. **260**(1995)187.
- [5] F. Senf, F. Eggenstein, and W. Peatman, Rev. Sci. Instrum. **63**(1992)1326.
- [6] E.L. Saldin, E.A. Schneidmiller and M.V. Yurkov, DESY Print, TESLA-FEL 96-07, Hamburg(1996)
- [7] P. Pierini and W. Fawley, Nucl. Instrum. and Methods **A375**(1996)332.